Bull. Mater. Sci., Vol. 31, No. 3, June 2008, pp. 455–459. © Indian Academy of Sciences.

Structure–property relationship of specialty elastomer–clay nanocomposites

ANIRBAN GANGULY, MADHUCHHANDA MAITI and ANIL K BHOWMICK*
Rubber Technology Centre, Indian Institute of Technology, Kharagpur 721 302, India

Abstract. The present work deals with the synthesis of specialty elastomer [fluoroelastomer and poly (styrene-*b*-ethylene-co-butylene-*b*-styrene (SEBS)]–clay nanocomposites and their structure–property relationship as elucidated from morphology studies by atomic force microscopy, transmission electron microscopy and X-ray diffraction and physico-mechanical properties. Due to polarity match, hydrophilic unmodified montmorillonite clay showed enhanced properties in resulting fluoroelastomer nanocomposites, while hydrophobic organo-clay showed best results in SEBS nanocomposites.

Keywords. Nanocomposites; nanoclays; fluoroelastomer; SEBS.

1. Introduction

Polymer nanocomposites are recognized as one of the most promising research areas in polymer science and technology in the 21st century. Worldwide market for polymer nanocomposites is expected to grow at an average annual rate of 18·4% to reach US$211 million by 2008 (BCC research 2007). Polymer-layered silicate nanocomposites are the foremost members of such nanocomposites which have exhibited great promise for industrial applications due to their ability to display synergistically advanced properties with relatively small amounts of clay loading (e.g. 1–5 wt%) (Usuki *et al* 1993; Giannelis *et al* 1999; Krishnamoorti *et al* 2001; Pinnavaia and Beall 2001; Roy and Okamoto 2003). From our laboratory, we have reported a number of polymer nanocomposites with unique properties (Pramanik *et al* 2003; Sadhu and Bhowmick 2003; Bandyopadhyay *et al* 2004; Sadhu and Bhowmick 2004, 2005; Sengupta *et al* 2005; Ganguly *et al* 2006, 2007; Maiti and Bhowmick 2006a, b, c). In this study, unmodified (MMT) and organically modified (CL) montmorillonite nanoclays having a 2 : 1 tetrahedral–octahedral layer structure (TOT), high aspect ratio, high cation-exchange capacity and self-assembling behaviour via specific interactions to form a stacked arrangement have been chosen to prepare fluoroelastomer and block copolymer [poly (styrene-*b*-ethylene-co-butylene-*b*-styrene (SEBS)] based nanocomposites. Their structures have been elucidated by many sophisticated techniques including atomic force microscopy, transmission electron microscopy and correlated with the X-ray diffraction, mechanical and dynamic mechanical properties.

*Author for correspondence (anilkb@rtc.iitkgp.ernet.in)

2. Experimental

2.1 *Materials*

Polymers chosen in this investigation were fluoroelastomer, Viton B-50, a 68% fluorine containing terpolymer of vinylidene fluoride, hexafluoropropylene, tetrafluoroethylene (F), Mooney Viscosity, ML_{1+10} at 120°C = 39 and poly [styrene-*b*-(ethylene-co-butylene)-*b*-styrene (SEBS)] having 30% styrene content, with Mn = 57,000.

Nanofillers: unmodified sodium montmorillonite clay (MMT) and organically modified (Na^+ cation-exchanged by long chain quaternary ammonium ion) clay (Sadhu and Bhowmick 2004; Ganguly *et al* 2006; Maiti and Bhowmick 2006a) and Cloisite 20A (CL) were procured from Southern Clay Products, TX, USA.

2.2 *Preparation of specialty rubber–clay nanocomposites*

Solvent cast method was employed to synthesize rubber–clay nanocomposites. Fluroelastomer was dissolved in methyl ethyl ketone (20 wt% solution) while SEBS was dissolved in toluene. Dispersed nanoclay was then added to respective elastomer solution as per the procedures described in our earlier publications (Sadhu and Bhowmick 2003, 2004; Ganguly *et al* 2006; Maiti and Bhowmick 2006a). After stirring for 2 h, nanocomposite solution was cast on levelled glass plate and dried slowly for 2 days.

2.3 *Characterization procedures*

2.3a *Atomic force microscopy (AFM)*: Multi mode atomic force microscope with a Nanoscope IIIa controller

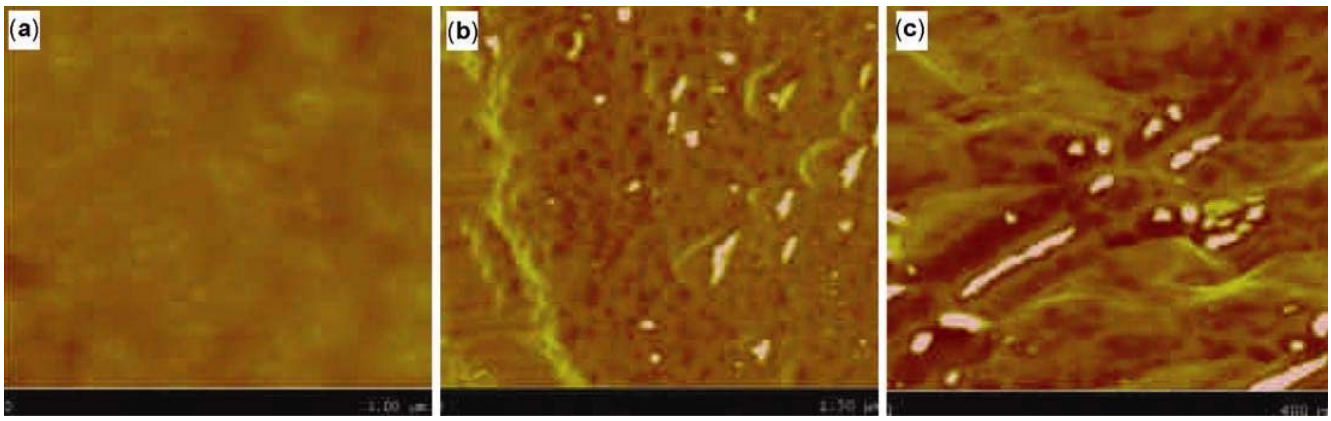

Figure 1. Tapping mode AFM phase image of (**a**) neat F and nanocomposites, (**b**) F-MMT4 and (**c**) F-CL4.

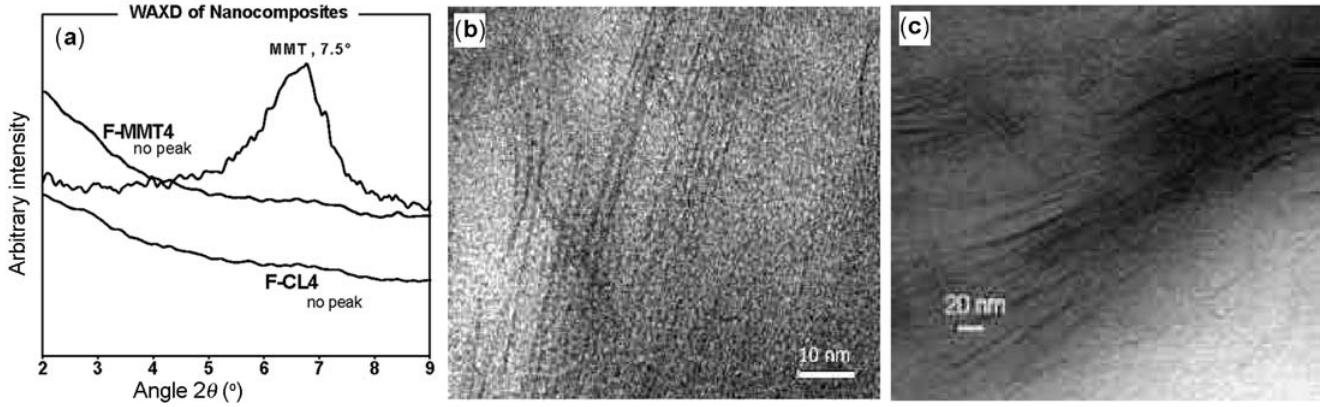

Figure 2. (**a**) XRD diffractogram of nanocomposites with MMT clay and TEM micrograph of (**b**) F-MMT4 and (**c**) F-CL4.

by Digital Instruments Inc. (Veeco Metrology Group), Santa Barbara, CA, USA, was used for AFM studies. The tapping mode was employed to analyse the attributes of the lamellar phase characteristics in different processes of nanocomposite preparation, differences in the topographical features in the presence and absence of dispersed nanofillers.

2.3b *Transmission electron microscopy (TEM)*: The samples for transmission electron microscopic analysis were prepared by ultracryo-microtomy using a Leica Ultracut UCT (Wien, Austria). Freshly sharpened glass knives with a cutting edge of 45° were used to get the cryosections of 50–70 nm thickness at a sub-ambient temperature of –80°C using a JEOL 2010, Japan TEM, operating at an accelerating voltage of 200 kV.

2.3c *X-ray diffraction studies (XRD)*: For the characterization of the rubber nanocomposites, XRD studies were performed using a PHILIPS X-PERT PRO diffractometer in the range $2\theta = 2$–$9°$ and Cu-target ($\lambda = 0{\cdot}154$ nm). Then, d-spacing of the clay particles was calculated using the Bragg's law

$$n\lambda = 2d\sin\theta.$$

2.3d *Dynamic mechanical thermal analysis (DMTA):* The dynamic mechanical spectra of the samples were obtained by using a DMTA IV (Rheometric Scientific, New Jersey, USA) dynamic mechanical thermal analyser. The sample specimens were analysed in tensile mode at a constant frequency of 1 Hz, a strain of 0·01% and temperature range from –80 to 80°C at a heating rate of 2°C/min.

2.3e *Mechanical properties*: Stress–strain experiments were carried out as per the ASTM D 412 method in a Universal Testing Machine (Z010, Zwick GmbH, Ulm, Germany) at a crosshead speed of 500 mm/min at room temperature (25 ± 2°C).

3. Results and discussion

3.1 *Fluoroelastomer–clay nanocomposites*

In the first part of present study, topographic and phase imaging in tapping mode atomic force microscopy was

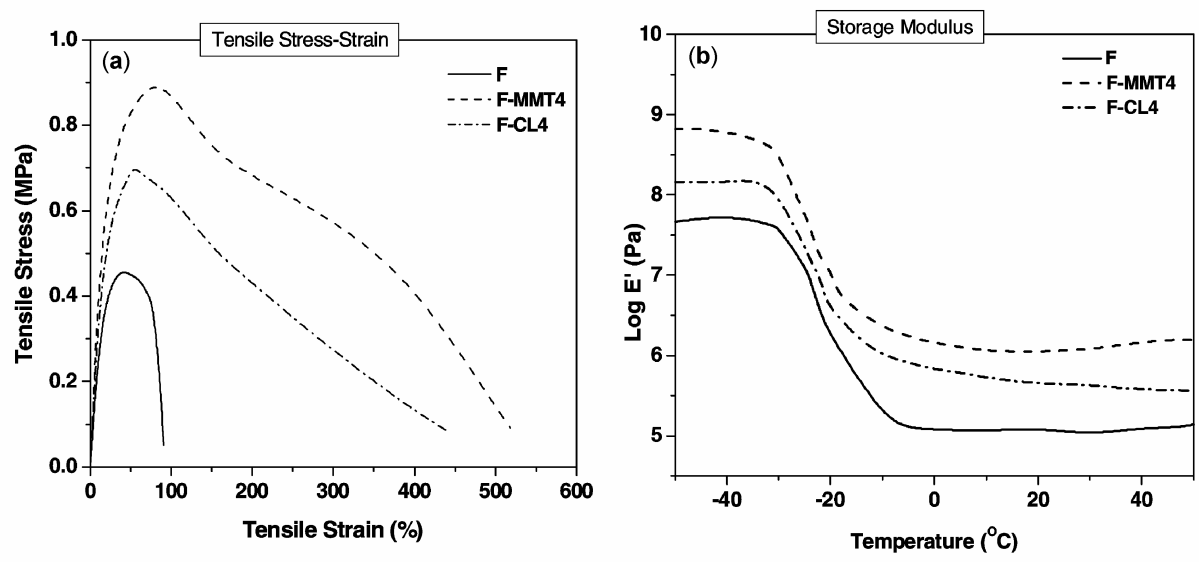

Figure 3. (**a**) Stress–strain curve and (**b**) logE' vs temperature plot of different fluoroelastomer nanocomposites.

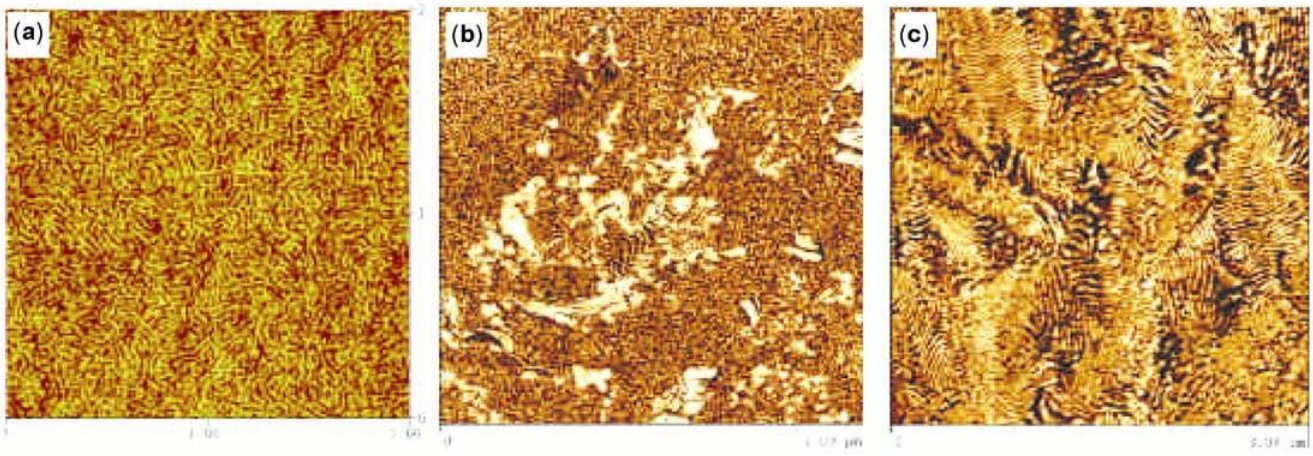

Figure 4. Atomic force microscopic phase images of (**a**) neat SEBS, (**b**) agglomerated SEBS–MMT4 composite and (**c**) exfoliated SEBS–CL4 nanocomposite.

performed to investigate the size of clay-platelets, the polymer–filler interface, and spatial distribution of the nanoclays (unmodified and modified clays) in the fluoroelastomer. The phase images (figure 1) of the unmodified clay filled (F-MMT4) and modified clay filled (F-CL4) nanocomposites revealed that the width of clay particles was lower in the case of the unmodified clay filled system (10±3 nm) than that of modified system (15 ± 2 nm).

The absence of characteristics peak (at 7·5° for MMT nanoclay) in the region 2–10° in XRD as shown in figure 2a indicates the total dispersion and delamination (exfoliation) of fine nanoclay layers in the matrix. Interestingly, the polymer clearly is able to exfoliate both the unmodified and modified clays as evident from X-ray diffraction studies (figure 2a). But the particle size is much lower in the case of F-MMT4 and distribution is also better in this particular sample as shown in TEM micrograph (figures 2b–c). This is in accordance with the AFM morphological results.

This may be due to better polymer–filler interaction in the case of the polar unmodified clay. The results of AFM characterization are also in good agreement with mechanical and dynamic mechanical properties. Both the studies reveal that F-MMT4 shows higher maximum stress and storage modulus than that of F-CL4 (figures 3a–b). There are 100 and 52% improvements in maximum stress, 151 and 83% in 100% modulus in the case of F-MMT4 and F-CL4, respectively compared to the control fluoroelastomer, F. The increase in storage modulus at room temperature and shift of tan δ peak towards positive temperature in the case of F–MMT4 is more compared to F–CL4 and F due to better interaction between

Table 1. Mechanical properties of SEBS and its clay nanocomposites.

Sample	Modulus (MPa)		Tensile strength (MPa)	Elongation at break (%)
	50%	300%		
SEBS	2·6	7·0	23·8	520 ± 10
SEBS–MMT4	2·2	8·2	24·2	550 ± 10
SEBS–CL4	3·5	11·0	31·6	580 ± 15

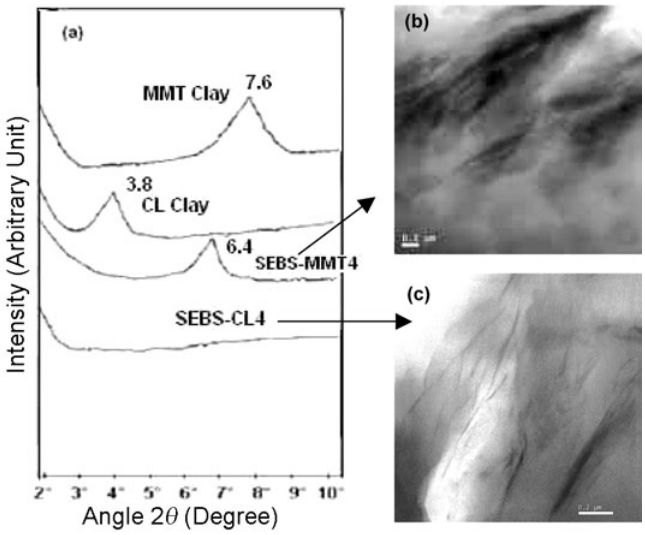

Figure 5. (**a**) X-ray diffractograms and transmission electron micrographs of (**b**) agglomerated SEBS–MMT4 composite and (**c**) exfoliated SEBS–CL4 nanocomposites.

the unmodified clay and the polar rubber matrix. This may be due to the presence of polar groups on the surface of MMT which attract the fluorocarbon elastomers having $C^{\delta+}$–$F^{\delta-}$ bonds. The results have also been explained with the help of thermodynamics and wetting behaviour of the clays (Maiti and Bhowmick 2006a).

3.2 *SEBS–clay nanocomposites*

In the second part of study, the phase detected images in the tapping mode atomic force microscopy exhibited a well-ordered phase separated morphology (figure 4) consisting of bright nano-phasic domains corresponding to hard component and darker domains corresponding to softer rubbery ethylene-co-butylene (PEB) lamella for a neat triblock copolymer poly [styrene-*b*-(ethylene-co-butylene)-*b*-styrene (SEBS)]. This lamellar morphology gives a domain width of 19–23 nm for bright styrenic nanophase and 12–15 nm for darker ethylene-co-butylene phase of SEBS (figure 4a). On incorporation of 4 wt% MMT clay into SEBS, agglomerated structure is obtained in SEBS–MMT4 (figure 4b). Due to proper interaction with CL nanoclay, SEBS lamella width (figure 4c) has been found to increase in the resulting nanocomposite (Ganguly *et al* 2007). The best exfoliation is demonstrated by SEBS–CL4 nanocomposite (figure 4c), where fine clay layers are dispersed all through the matrix as a result of which the characteristics peak for clay disappears in the region of 2–10° in XRD. Studies by XRD and TEM (figure 5(a–c)) corroborate the AFM results.

Very stiff nature of the clay particles in the matrix has been analysed from the almost zero pull-off and snap-in force in the force-distance analyses of SEBS based nanocomposite in single point- and force-volume modes by AFM force study (force-deflection curves were recorded by plotting the cantilever deflection against movement of piezo in *z*-direction) following the Hook's law ($F = k.\ Z$) (Ganguly *et al* 2006, 2007; Maiti and Bhowmick 2006b).

The higher polymer–filler interaction is a result of exfoliation/intercalation in this nanocomposite as revealed from X-ray diffractogram, AFM and TEM micrographs (figures 4–5). Due to agglomerated thick-stack structure of MMT clays in SEBS–MMT4 as shown from AFM phase image in figure 4b and TEM bright field image in figure 5b, little improvement in tensile strength is observed in this composite, while SEBS–CL4 registers much higher increment of 33 and 57% in tensile strength and modulus, respectively compared to the neat SEBS system (table 1). Mechanical and dynamic mechanical thermal properties are observed to be best with SEBS–CL4 nanocomposites (figure 6). Significant improvements in mechanical properties such as tensile strength, modulus and elongation at break were achieved in this nanocomposite.

SEBS–CL4 shows markedly improved dynamic storage modulus ($\log E'$) both in the glassy as well as in the rubbery regions (figure 6a) as compared to the control SEBS and SEBS–MMT4 nanocomposite. It is possibly due to the better polymer–organically modified clay interaction. It is also revealed from figure 6b that both the low temperature rubbery T_g for ethylene butylene part and higher temperature T_g for polystyrene of SEBS shift towards each other with lowering of peak heights indicating a compatibilizing effect in the said SEBS–CL4 nanocomposite.

4. Conclusions

Montmorillonite nanoclay based nanocomposites were prepared from two types of specialty elastomers—polar fluoroelastomer and non-polar SEBS. Fluoroelastomer showed exfoliations with both the unmodified (MMT)

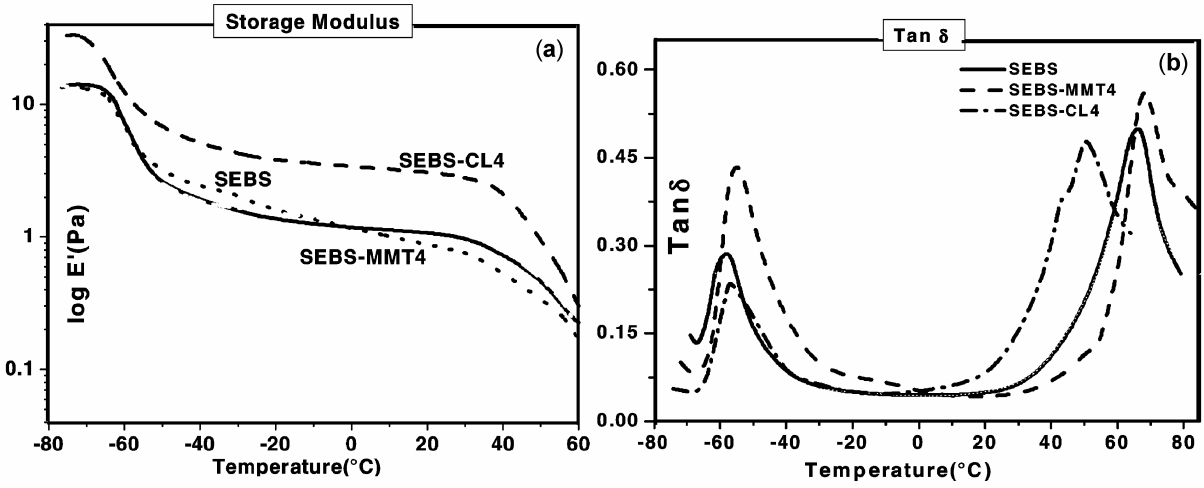

Figure 6. (**a**) Storage modulus vs temperature and (**b**) tan δ vs temperature plots for SEBS and SEBS–clay nanocomposites.

and modified clays (CL), while SEBS demonstrated preferential affinity towards modified CL clay as evident from physico-mechanical, microstructure by XRD and morphological investigations. Hydrophilic MMT nanoclay showed affinity towards fluoroelastomer while hydrophobic CL nanoclay had the same with SEBS for polarity match. Thus, enhanced mechanical and dynamic mechanical properties were achieved in the case of F–MMT4 and SEBS–CL4 nanocomposites inferred from exfoliated morphology as evident from X-ray diffraction, atomic force and transmission electron microscopic studies.

Acknowledgements

The authors thankfully acknowledge DST, New Delhi, for partial funding for procurement of atomic force microscopy. One of the authors (AG) acknowledges AICTE, New Delhi, for financial help in the form of a scholarship grant under NDF category.

References

Bandyopadhyay A, De Sarkar M and Bhowmick A K 2004 *Rubber Chem. Technol.* **77** 830

Ganguly A, De Sarkar M and Bhowmick A K 2006 *J. Appl. Polym. Sci.* **100** 2040

Ganguly A, De Sarkar M and Bhowmick A K 2007 *J. Polym. Sci.: Part B: Polym. Phys.* **45** 52

Giannelis E P, Krishnamoorti R and Manias E 1999 *Adv. Polym. Sci.* **138** 108

http://www.bccresearch.com/editors/rp-234r.html

Krishnamoorti R, Silva A S and Mitchell C A 2001 *J. Chem. Phys.* **115** 7175

Maiti M and Bhowmick A K 2006a *J. Polym. Sci.: Part B: Polym. Phys.* **44** 162

Maiti M and Bhowmick A K 2006b *Polymer* **47** 6156

Maiti M and Bhowmick A K 2006c *J. Appl. Polym. Sci.* **101** 2407

Pinnavaia T J and Beall G W 2001 *Polymer–clay nanocomposites* (Chichester, England: John Wiley & Sons Ltd)

Pramanik M, Srivastava S K, Samantaray B K and Bhowmick A K 2003 *J. Appl. Polym. Sci.* **87** 2216

Roy S S and Okamoto M 2003 *Prog. Polym. Sci.* **28** 1539

Sadhu S and Bhowmick A K 2003 *Rubber Chem. Technol.* **76** 0860

Sadhu S and Bhowmick A K 2004 *J. Polym. Sci. Part B: Polym. Phys.* **42** 1573

Sadhu S and Bhowmick A K 2005 *J. Mater. Sci.* **40** 1633

Sengupta R, Bandyopadhyay A, Sabharwal S, Chaki T K and Bhowmick A K 2005 *Polymer* **46** 3345

Usuki A, Kojima Y, Kawasumi M, Okada A, Fukushima Y, Kurauchi T and Kamigaito O 1993 *J. Mater. Res.* **8** 1174